PROCEEDINGS, 41st Workshop on Geothermal Reservoir Engineering
Stanford University, Stanford, California, February 22-24, 2016
SGP-TR-209

# Static Formation Temperature Prediction based on Bottom Hole Temperature

Changwei. Liu, Youguang Chen and Kewen Li

China University of Geosciences (Beijing)

29 Xueyuan Road, Beijing, China

changweiliu@outlook.com

**Keywords:** static formation temperature, shut-in time, modified model.

## ABSTRACT

The static formation temperature (SFT) is required to determine the thermophysical properties and production parameters in geothermal and oil reservoirs. However, the SFT is not easy to be obtained by both experimental and physical methods. In this paper, a mathematical approach to predicting SFT based on a new model describing the relationship between bottom hole temperature (BHT) and shut-in time was proposed. The unknown coefficients of the model were derived from least squares fit by Particle Swarm Optimization (PSO) algorithm. Besides, the ability to predict SFT based on a small number of BHT data (such as first 3, 4, or 5 ones of a data set) was evaluated. The accuracy of the proposed method to predict SFT was testified with a deviation percentage less than $\pm 4\%$ and high values of regression coefficient $R^2$ $(> 0.98)$. The proposed method could be used as a practical tool to predict SFT in both geothermal and oil wells.

## 1. INTRODUCTION

Drilling deep borehole is needed for the exploitation of geothermal energy (Saito et al., 1998). The borehole drilling is a complicated process in which a constant thermal anomaly (added to a circulating drilling mud) affects the static formation temperature (SFT) around the borehole (Fomin et al., 2013). Determining SFT at any depth needs a certain length of time, in which the bottom-hole temperature (BHT) and shut-in time measurements are conducted (Santoyo et al., 2000). Measuring BHT can be costly due to the usage of sophisticated log equipment and the necessity to stop the wellbore drilling (Wisian et al., 1998).

Appropriate estimation of SFT is required for several applications: (1) determination of geothermal heat flow; (2) analysis of well logs; (3) estimation of geothermal potential; (4) evaluation of in-situ thermophysical formation properties (Bassam et al., 2010); (5) determination of hydrocarbons properties in petroleum systems (Melton and Giardini, 1984; Armstrong et al., 1996; Matthai and Stephan, 2008).

Estimation of SFT is usually achieved by analytical methods and numerical simulation methods. Most of the analytical methods are based on the constant linear and cylindrical heat source models. Some analytical methods most commonly used to estimate SFT are: (1) Honer-plot method (HM method) or the line-source method (Dowdle and Cobb, 1975); (2) the Kutasov-Eppelbaum method (KEM method) or the generalized Honer method (Kutasov and Eppelbaum, 2005); (3) the Manetti method (MM method) or the cylindrical source with a conductive heat flow method (Manetti, 1973); (4) the Hansan and Kabir method (HK method) or the cylindrical heat source with a conductive-convective heat flow method (Hasan et al., 1994); (5) the Bernnand method (BM method) or the radial source with a conductive heat flow method (Brennand, 1984); (6) the spherical and redial heat flow method (SRM) proposed by Ascencio et al. (1994); (7) the Leblanc method (LM method) or the cylindrical source with a conductive heat flow method (Lech, 2012).

The values of SFT are obtained from those methods by using BHT and shut-in time data as input data, as well as the linear or nonlinear regression models as solutions (Espinoza-Ojeda et al., 2011). Large errors are likely to be found when these methods are applied to BHT data to predict SFT. The error sources are: (1) unrealistic models proposed to describe the drilling process; (2) heat transfer models based on simple assumptions; (3) measurement errors of BHT data; (4) total uncertainties of SFT estimation (Wong-Loya et al., 2012).

Numerical simulation is another method to estimate SFT, which can also be applied to determine geothermal gradients and describe the thermal history (Tragesser et al., 1967). For example, Garcia et al. (1988) developed a numerical simulator entitled TEMLOPI for estimating the transient temperature distribution in a wellbore and the surrounding rock formation. Application to well Az-29 from the Los Azufres Mexican geothermal field shows satisfactory results. The simulator could be used by drilling engineers to determine the optimal design of cement slurries and setting times of the cements during the well construction process.

Both of those analytical and numerical simulation methods have some limitations: (1) excessive amount of data are needed besides BHT and shut-in time, such as thermophysical and transport properties of the wellbore (drilling and cementing materials), formation and rock materials. Those data are rarely available, which limits the usage of those methods. (2) the accurate circulation time is usually unknown or difficult to determine under drilling conditions.

A reliable and practical tool to estimate SFT is still required in the geothermal and petroleum industries. In this paper, a mathematical function was proposed to correlate BHT and shut-in time. The coefficients of the function were obtained from Particle Swarm Optimization (PSO) algorithm based on the least squares fit target.

PSO is a stochastic, population-based optimization method introduced by Kennedy and Eberhart (Kennedy and Eberhart, 1995). It belongs to the family of swarm intelligence computational techniques and is inspired by social interaction in human beings and animals (especially bird flocking and fish schooling). PSO optimizes a problem by having a population of candidate solutions, dubbed particles here, and moving these particles around in the search-space according to simple mathematical formulae over the particle's position and velocity. Each particle's movement is influenced by its local best known position but, is also guided toward the best known positions in the search-space, which are updated as better positions are found by other particles. PSO algorithm has been used in many numerical solution problems and shows its wide applicability (Chen et al., 2010; Ziari and Jalilian, 2012; Mahor and Rangnekar, 2012).

PSO has some advantages in solving optimization problems: (1) few parameters to be tuned by user; (2) high accuracy; (3) less affected by initial solutions comparing with other algorithms; (4) fast convergence; (5) easy codes due to the simple underlying concepts; (6) no requirement for preconditions such as continuity or differentiability of objective functions (Jordehi, 2015).

## 2. METHODOLOGY

In this section, a function correlating BHT and shut-in time was derived to fit the BHT data and estimate SFT. The coefficients of this function can be obtained from least squares fit method using Particle Swarm Optimization (PSO) algorithm. Besides, other methods were also introduced and used to compare with the new one. Statistical tests were applied to evaluate the validity of those predicting methods.

### 2.1 Method Development

#### 2.1.1 Function derivation

Horner method for obtaining the static formation temperature has been widely used in oil and gas industry (Dowdle and Cobb, 1975). This analytical method is based on assumption that the thermal effect of drilling is a constant linear heat source. The approximation solution is given by:

$$\mathrm{BHT(t)} = \mathrm{T}_{HM} + (b_{HM}) \cdot \log\{(t_C + t)/t\} \tag{1}$$

Where $T_{HM}$ is static formation temperature, $\log\{(t_C + t)/t\}$ is known as the Dimensionless Horner Time (DHT), $t_c$ and $t$ are the circulation time before shut-in and the time elapsed since the circulation stops, respectively. One of the problems that Equation (1) has is the inconsistency of the boundary conditions. BHT approaches to the static formation temperature, $T_{HM}$, when $t$ approaches to infinite, which is correct. However, BHT cannot be obtained when $t$ approaches or is equal to zero. This problem may also decrease the fitting goodness of the model. We propose the following mathematical model in order to solve the above problem that Equation (1) has. The modified model is expressed as:

$$\mathrm{BHT(t)} = \mathrm{a} + b \cdot \log\left\{\frac{1}{(1+c\cdot t)} + 1\right\} \tag{2}$$

Where $a$, $b$, and $c$ are constant, $a$ is actually equal to $T_{HM}$, which can be estimated using Equation (2) when shut-in time tends to infinity:

$$\widehat{\mathrm{SFT}} = \lim_{t\to\infty} \mathrm{BHT} = a \tag{3}$$

Equation (2) meets all of the boundary (time) conditions:

- when $t$ approaches to infinite, the maximum BHT is obtained:

$$\mathrm{BHT}_{max} = \mathrm{T}_{HM} = a \tag{4}$$

- when $t$ approaches to zero, the minimum BHT is obtained:

$$\mathrm{BHT}_{min} = a + b \cdot ln2 \tag{5}$$

One can see that the problem that Equation (1) has is solved in Equation (2). When the maximum and minimum of BHT are both decided, the shape of the BHT-time curve only depends on the values of c. The curve of the BHT-time function is illustrated in Figure 1. The equation can characterize the BHT-time function in a big scope, as shown in Figure 1.

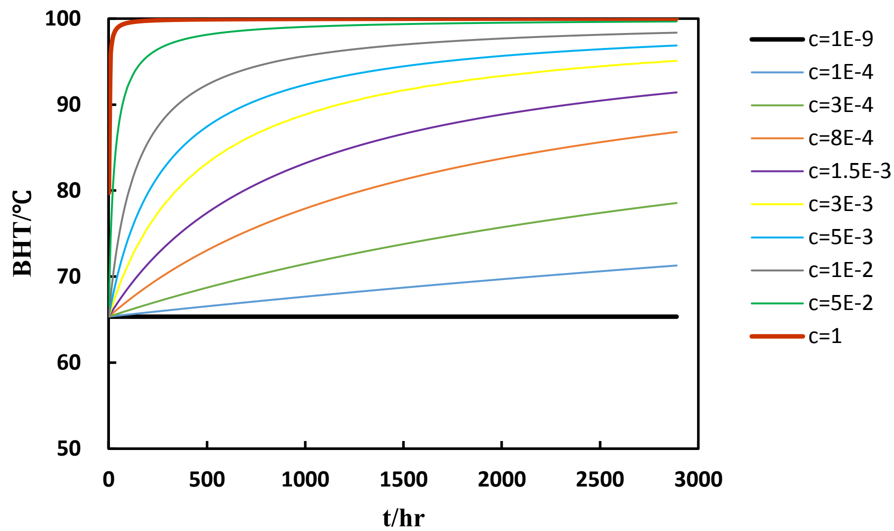


**Figure 1. Relationship between BHT and shut-in time where a=100, b=-50, and c varies from 1E-9 to 1.**

2.2.2 Solutions to the three parameters in the new function

In order to obtain the best fit of the equation, the least squares fit target is applied. Difference between the proposed function and the measured value of temperature is denoted by Q, which is obtained using the following equation:

$$\mathrm{Q} = \sum_{i=1}^{n}(\mathrm{BHT}_i - \mathrm{BHT}_{ci})^2 \quad (6)$$

where $\mathrm{BHT}_i$ is the measured BHT, $BHT_{ci}$ is the BHT calculated by Equation (2).

The least squares fit method requires the minimization of Q. Here we used Particle Swarm Optimization (PSO) algorithm to obtain the best fitting coefficients of $a$, $b$, and c that yields the minimum value of X.

The position and velocity of $i^{th}$ particle are respectively denoted by $X_i$ and $V_i$, the best position found by each particle is referred to as its personal best. For $i^{th}$ particle, the position vector of personal best is denoted by $Pi$ and its objective value is denoted by $P_{best}$. The best position found by the swarm is referred to as swarm best, global best or leader. It is denoted by $P_g$ and its objective is denoted by $g_{best}$. At each iteration of $t$, the positions and velocities of all particles are updated by Equations (7) and (8) which are called update equations (Jordehi, 2015).

$$V_i(t+1) = \omega V_i(t) + C_1 r_1 (P_i - X_i) + C_2 r_2 (P_g - X_i) \quad (i = 1,2, \ldots, N_P) \quad (7)$$

$$X_i(t+1) = X_i(t) + V_I(t+1) \quad (i = 1,2, \ldots, N_P) \quad (8)$$

where $\omega$ is inertia weight; $C_1$ is the cognitive acceleration coefficients, which prompts the attraction of the particle towards its own personal best; $C_2$is the social acceleration coefficients, which prompts the attraction of the particle towards the swarm best; $r_1$ and $r_2$ are two random numbers in [0,1].

A schematic of the solving process of the proposed method is depicted in Figure 3.

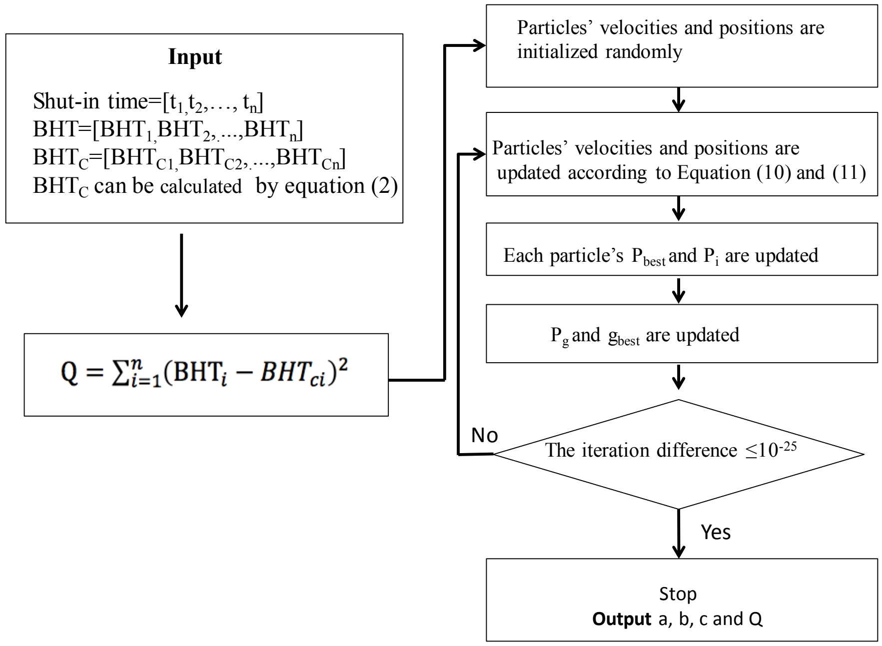


**Figure 2. The scheme of the solving process of the proposed method.**

**2.2 Existing methods**

2.2.1 Selection of the analytical methods

Some of the existing methods were discussed in this paper to compare with the proposed method. Three most commonly used analytical methods were introduced. The equations, analytical models and sources of these methods were listed in Table 1. Basically, two regression models were applied to obtain the coefficients in each analytical method.

**Table 1: A summary of the analytical methods used to compare in this paper.**

| Method | Physical model | Equation | Sources |
|---|---|---|---|
| Horner (HM) | Constant Linear heat source | $BHT(t) = T_{HM} + b_{HM} ln\left(\frac{t+t_c}{t}\right)$ (12) | Dowdle and Cobb (1975) |
| Manetti (MM) | Conductive cylindrical heat source | $BHT(t) = T_{MM} + b_{MM} ln\left(\frac{t}{t-t_c}\right)$ (13) | Manetti (1973) |
| Ascencio (SRM) | Spherical-radial heat flow | $BHT(t) = T_{SRM} + b_{SRM} ln\left(\frac{1}{\sqrt{t}}\right)$ (14) | Ascencio et al. (1994) |

2.2.2 Selection of the regression models

Two regression methods were used as regression models to obtain the coefficients in the three analytical methods: ordinary linear regression (OLR) model and quadratic regression (QR) model.

The general equation of this model is: $y = a + b \cdot x$, where *a* and *b* are the intercept and the slope of the fitted straight line (Espinoza-Ojeda et al., 2011).

The general equation of the QR model is given by: $y=a+bx+cx^2$, where *a*, *b* and *c* represent the polynomial coefficients (Espinoza-Ojeda et al., 2011).

**2.3 Statistical evaluation**

(1) Deviation percentages (DEV%): in order to test the estimation accuracy of SFT, the deviation percentages (DEV%) between SFT estimate and reported SFT value were used:

$$DEV\% = \left[\frac{(\widehat{SFT}-SFT)}{SFT}\right] \times 100 \quad (9)$$

where $\widehat{SFT}$ is the value of SFT estimate, SFT is the true SFT value reported in literature.

It should be noted that this evaluation test was not applied from data set without reported SFT (Data 7 and Data 8). The closer the DEV% to zero, the better the estimation of SFT.

(2) Regression coefficient ($R^2$): the regression coefficient ($R^2$) is applied for testing the fitting ability of each method. The value can be obtained from:

$$R^2 = 1 - \frac{\sum(y_i - \hat{y}_i)^2}{\sum(y_i - \bar{y})^2} \tag{10}$$

where $y_i$ is the measured value of BHT, $\hat{y}_i$ is the BHT estimate and $\bar{y}$ is the mean of the measured BHT values.

The fitting is more satisfactory if the value of $R^2$ is closer to 1.

(3) Residual sum of squares (RSS): the fitting results of each method can also be evaluated through the estimation of normalized residual sum of squares (RSS), which is given by the following equation:

$$\text{RSS} = \frac{\sum_{i=1}^{n}(y_i - \hat{y}_i)^2}{n} \tag{11}$$

where $y_i$ and $\hat{y}_i$ are the same as in Equation (11), $n$ is the total numbers of BHT in a data set.

In a data set, the smaller the value of RSS, the better the fitting results.

The goodness of fitting can be evaluated by DEV% and $R^2$. However, the comparison between different methods should be based on the whole accuracy and fitting ability of each method. To evaluate each method comprehensively, the following synthetic statistical parameter was also used.

(4) Theil inequality coefficient (TIC): TIC is applied to test the estimation accuracy comprehensively when only very a small number of BHT data are used. For each data set and each method used, the TIC values can be obtained:

$$\text{TIC} = \frac{\sqrt{\sum_{i=3}^{5}(\widehat{SFT}_i - SFT)^2}}{\sqrt{\sum_{i=3}^{5}\widehat{SFT}_i{}^2} + SFT} \tag{12}$$

where $\widehat{SFT}_i$ is the SFT estimated using $i$ data set.

The value of TIC is in [0, 1] and could be used to compare between different data sets. For each method, the closer the TIC to zero, the more accurate the method.

## 2.4 Data sources

Eight thermal recovery data sets were collected from the published literature for the accuracy and application tests:

1) Four synthetic data sets were selected from literature;

2) Four data sets logged in some boreholes from long logging work including geothermal and petroleum field data.

Those data sets were summarized in the Table 2.

It should be pointed out that Data 1 to Data 6 all have reported SFT values, which can be very useful to evaluate the proposed method and conduct the comparisons between different methods.

**Table 2: Summary of the BHT data sets used in this paper.**

| Data | Type | n | $t_c$ (hr) | Sources | Data name in this paper |
|---|---|---|---|---|---|
| SHBE | Synthetic data | 8 | 5 | Shen and Beck (1986) | Data 1 |
| CLAH | Synthetic data | 15 | 5 | Cao et al. (1988) | Data 2 |
| CJON | Synthetic data | 12 | 0.2 | Cooper and Jones (1959) | Data 3 |
| KJ-21 | Geothermal field data | 6 | 2.5 | Steingrimsson and Gudmundsson (1989) | Data 4 |
| SG | Geothermal field data | 12 | 3 | Schoeppel and Gilarranz (1966) | Data 5 |
| MOU | Synthetic data | 3 | 10 | Mou (2013) | Data 6 |
| DA-XIN | Geothermal field data | 40 | 5 | Da-Xin (1986) | Data 7 |
| UASM | Petroleum field data | 14 | 10 | Kutasov (1999) | Data 8 |

## 3. VALDATION OF THE PROPOSED MODEL

### 3.1 Accuracy of the SFT

For each data set, coefficients a, b and c were solved by PSO algorithm based on the least squares fit target. After applying Equation (2), the BHT data were recalculated at each shut-in time of the set. The DEV% between SFT estimate and reported SFT were obtained from Equation (9). Results of the comparison between data from literature and data estimated by our proposed method were depicted in Figure 3, in which the yellow circle represents the measured BHT values (reported BHT), the black dot represents the calculated BHT, the red full line represents the reported SFT, and the black dashed line represents the value of SFT estimate.

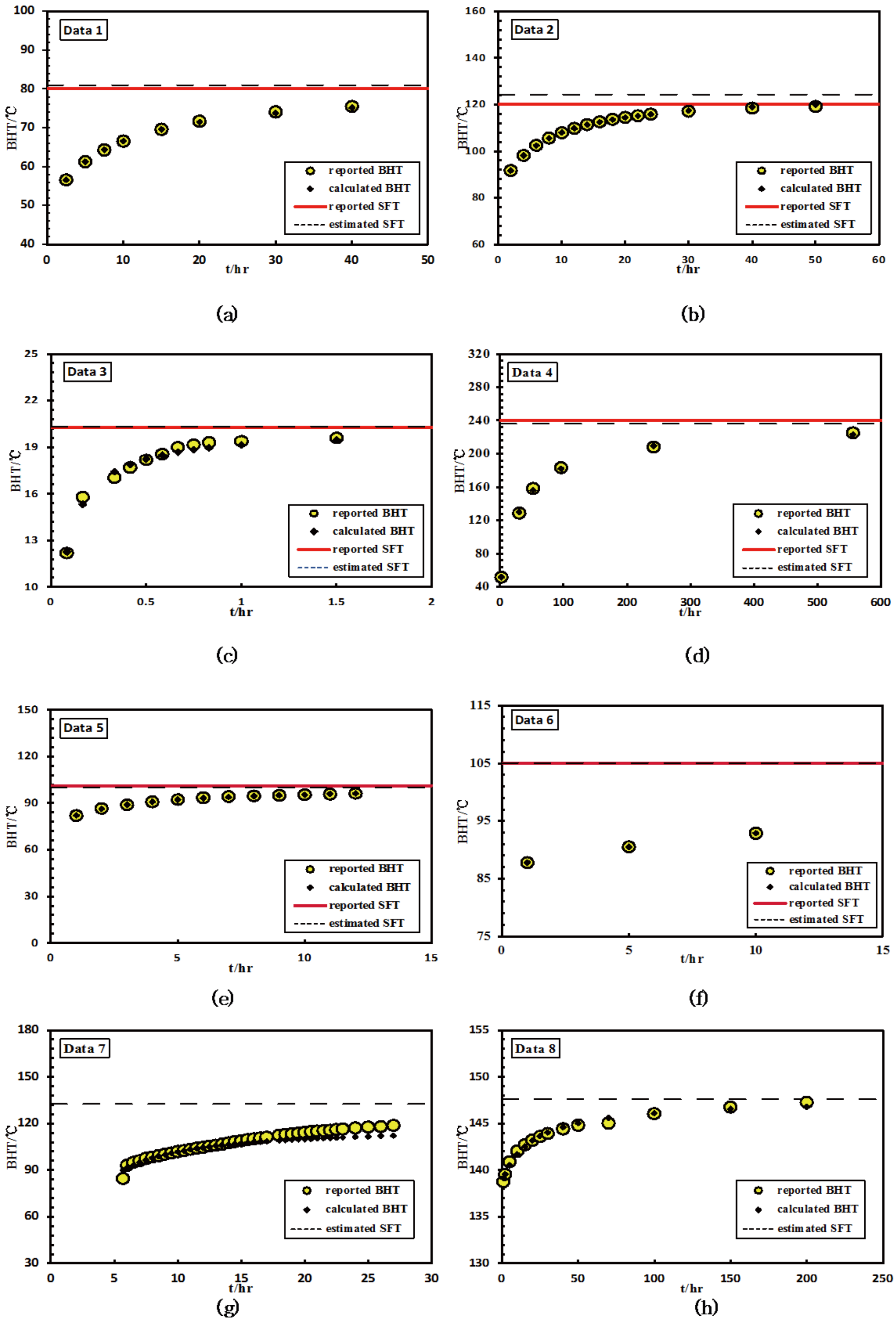


**Figure 3: Comparison between the BHT and SFT estimates obtained from proposed method and data from literatures.**

As for the synthetic set of Data 1, the SFT value estimated by the proposed method was 80.99°C, which is in agreement with the true SFT of 80°C. The error is 1.24%. The SFT estimated in Data 2 is about 4°C higher than the true value (120°C), with an acceptable deviation percentage of 3.52%. For those data sets from the well-logging (Data 4 and Data 5), the deviation percentages fall into the range of -2% to 1%. Data 6 were recorded at three shut-in times. Even so, SFT value (105.296°C) was estimated accurately in Data 6 by the proposed method, with a deviation percentage of 0.28% with the reported SFT value (105°C).

Figure 4 shows the comparison between estimated SFT values using the proposed method and true SFT values of the 6 data sets with the true SFT values ranging from 20.25 to 240 °C, the last shut-in time from 1.5hr to 600 hr. The number of the data set varies from 3 to 15. The DEV% of each data set is in [-2%, 4%], a satisfactory range as a practical predicting tool.

### 3.2 Fitting results

The regression coefficients $R^2$ determined by Equation (10) and the normalized RSS by Equation (11) were calculated for all data sets using the proposed method. The calculation results were presented in Table 3, and the BHT values calculated by the proposed method were shown in Figure 3. As for Data 1 and Data 2, the values of $R^2$ are both greater than 99.9%, which indicates the proposed method can fit the BHT data accurately. As for those BHT data sets recorded from well-logging work, the proposed method also showed good fitting ability because $R^2$ of each data set is more than 98%. Based on the matching results, the proposed method seems to provide acceptable correlations between BHT and shut-in time.

**Table 3: Results of each data set using the proposed method.**

| NO. | coefficients of the Proposed method | | | STF | SFT | DEV% | $R^2$ | RSS |
|---|---|---|---|---|---|---|---|---|
| | a | b | c | (reported) | (estimated) | | | |
| Data 1 | 81.000 | 45.960 | 0.172 | 80.000 | 81.000 | 1.249 | 1.000 | 0.025 |
| Data 2 | 124.232 | 63.459 | 0.243 | 120.000 | 124.232 | 3.527 | 0.999 | 0.089 |
| Data 3 | 20.327 | 30.865 | 28.299 | 20.250 | 20.327 | 0.380 | 0.987 | 0.073 |
| Data 4 | 236.084 | 280.837 | 0.039 | 240.000 | 236.084 | -1.632 | 0.999 | 2.243 |
| Data 5 | 100.132 | 21.111 | 0.694 | 101.111 | 100.132 | -0.968 | 0.999 | 0.026 |
| Data 6 | 105.296 | 26.481 | 0.067 | 105.000 | 105.296 | 0.282 | 1.000 | 0.000 |
| Data7 | 132.459 | 133.588 | 0.289 | N/A | 132.459 | N/A | 0.979 | 11.053 |
| Data 8 | 147.600 | 12.809 | 0.071 | N/A | 147.600 | N/A | 0.979 | 0.085 |

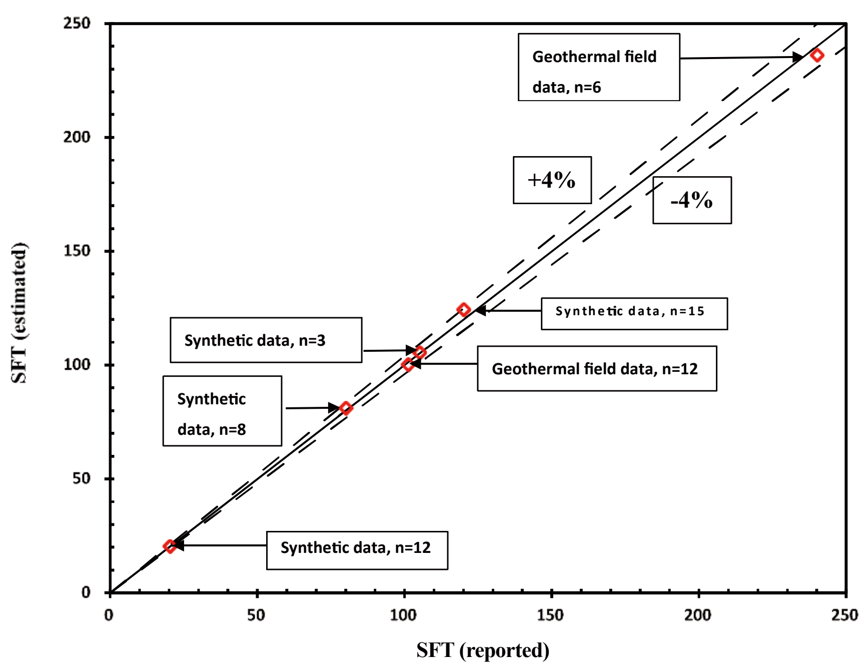


**Figure 4: Comparison between the SFT estimates using the proposed method and reported SFT values.**

In addition, comparisons with other methods between the SFT estimates and reported SFT values were made and the results are shown in Table 4. It is obvious that the SFT values predicted by the proposed method is much better than the existing models.

**Table 4：Comparison with other methods between the SFT estimates and reported SFT values.**

| | HM | | MM | | SRM | | Proposed Method | Reported SFT |
|---|---|---|---|---|---|---|---|---|
| | OLR | QR | OLR | QR | OLR | QR | | |
| Data1 | 75.871 | 79.372 | 74.713 | 77.936 | 77.362 | 86.914 | 80.999 | 80 |
| Data2 | 119.66 | 123.26 | 117.45 | 121.15 | 125.63 | 131.91 | 124.231 | 120 |
| Data3 | 20.328 | 18.981 | 20.003 | 21.302 | 22.132 | 19.499 | 20.327 | 20.25 |
| Data4 | 187.6 | 223.5 | 220.64 | 230.65 | 207.39 | 260.87 | 236.084 | 240 |
| Data5 | 98.449 | 100.07 | 97.048 | 98.257 | 99.858 | 106.16 | 100.133 | 101.111 |
| Data6 | 94.261 | 98.535 | 94.971 | N/A | 94.334 | 101.23 | 105.296 | 105 |

## 4 APPLICATIONS IN THE CASES WITH A SMALL NUMBER OF DATA POINTS

In this section, the fitting ability of the proposed method is tested in the cases with a small number of BHT data. Three other analytical methods with two different regression models mentioned in Section 2 were applied for comparison. The first 3, 4 or 5 points of each data set were applied to estimate SFT using different analytical methods and the proposed method. The results are discussed in this section.

Figures 5 and 6 presents the SFT estimation results using different methods when the first 3, 4, 5 points or all data of each set (DN 3, DN4, DN 5, and DN ALL) were used, respectively. The red solid line in each figure represents the true value of SFT in each data set, whereas the black dashed line represents the SFT values with the DEV% of 5% and -5% of the true SFT value, respectively. The circles in Figure 5 and the diamonds in Figure 6 represent the results of SFT estimated using different methods. Note that the red diamonds in Figure 6 represents the SFT data estimated using the new method. The results of deviation percentages between each estimate with the reported SFT value were listed in Table 4 for reference. The SFT estimates discussed here were obtained using 7 methods respectively and the range of [SFT-5% SFT, SFT +5% SFT] was called “acceptable range”.

After comparing the SFT estimates with the reported SFT values, it can be observed in Figure 5 that the SFT values estimated by Horner Method (HM) when OLR model was applied were typically underestimated in data sets except for Data 3. Besides, the aspheric heat-flow method (SRM) with OLR model was likely to overestimate the SFT, which was also mentioned in (Wong-Loyal et al., 2012). As for the regression models, results showed that SFT values estimated by using ordinary linear regression model were less than those by quadratic regression model in Figure 5. This observation was also reported in other literature (Espinoza-Ojeda et al., 2011; Wong-Loya et al., 2012).

For Data 1 and Data 2, the proposed method is the only method that all SFT estimates were lie in the acceptable range. Except for the proposed method, HM method with QR model and MM method with QR model were also good estimating methods, as shown in Figures 5 (a) and (b). However, the SFT estimates using those two method from first 3 points of Data 1 were both out of the acceptable range.

For Data 3, the estimation results of three methods were all in the acceptable range. Those three methods are HM method with OLR model, MM method with OLR model, and the proposed method. Both SRM methods with OLR and QR models estimated the SFT poorly.

For Data 4, the SFT estimated by each method from DN 3 was out of the acceptable range. The proposed method was the only one lied in the acceptable range (estimates from DN 4, DN 5 and DN ALL). Except for one SFT estimated by MM method with QR model from DN ALL was in the acceptable range, all estimates using other methods were unacceptable.

For Data 5, the predicting results of the proposed method and other four methods all lied in the acceptable range. For Data 7 without the reported SFT value, the predicting stability of each method can still be seen in Figure 5 (f). The estimates obtained from HM method with OLR model and SRM method with OLR model were unstable, with the range of 63.77 $^{o}$C and 99.74 $^{o}$C respectively. And the proposed method as well as the MM method with OLR model can estimate SFT stably.

Except for SRM method with QR model and the proposed method, the estimates of other methods were likely to be underestimated when only the first 3, 4 or 5 points of the data set were used. While the estimates by SRM method with QR model were more likely to be overestimated. However, estimates obtained from the proposed method were likely to distribute on both sides of the reported SFT value (red full lines in Figure 5), which is also a sign of the advantage of the proposed method.

Based on the statistical tests and the above analysis, the proposed method can estimate SFT accurately and stably in the cases with few data.

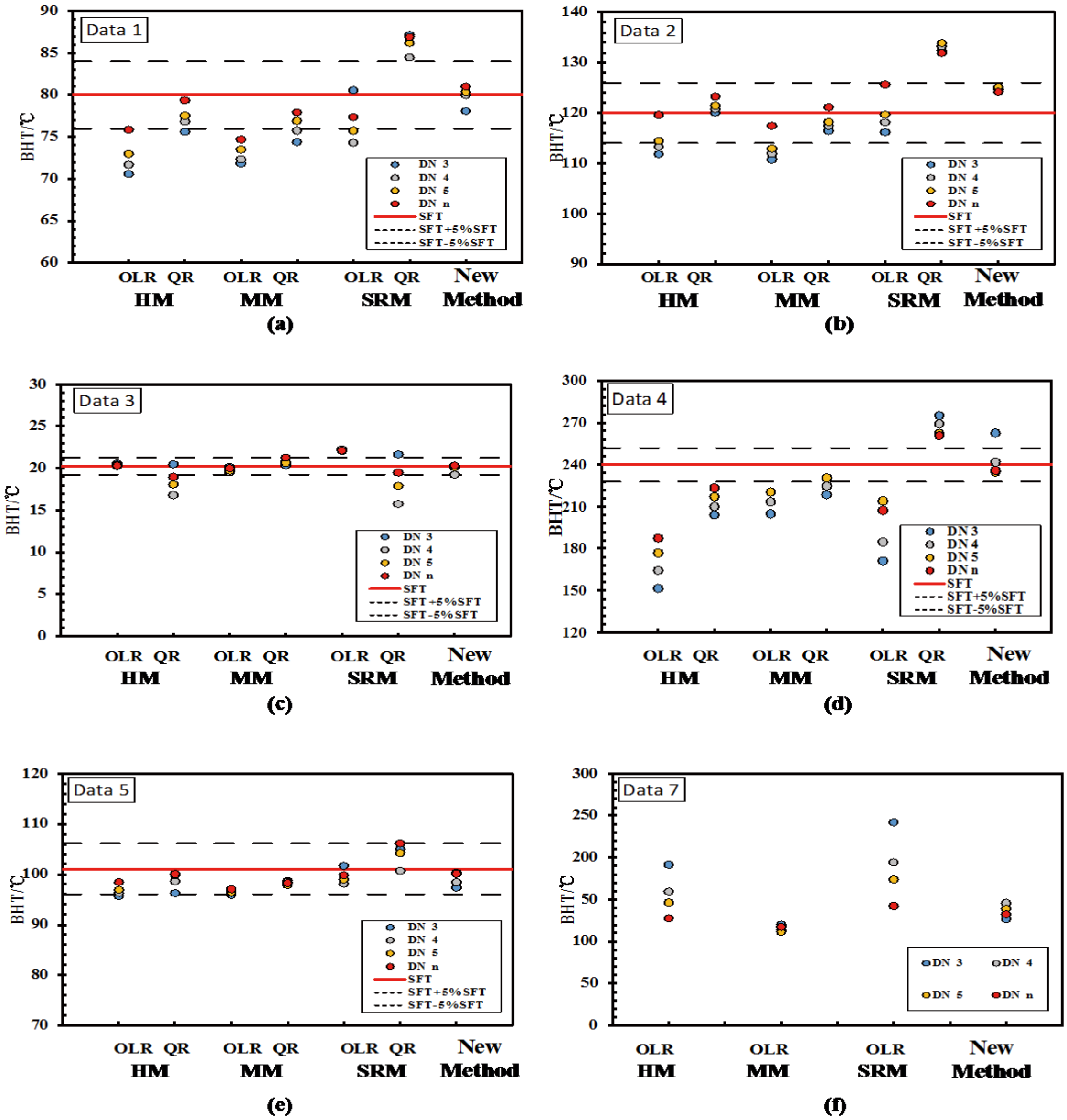


**Figure 5: SFT estimates of each method using the first 3, 4 5, or n points of a data set, respectively. (DN 3 represents that the first 3 points of a data set were used).**

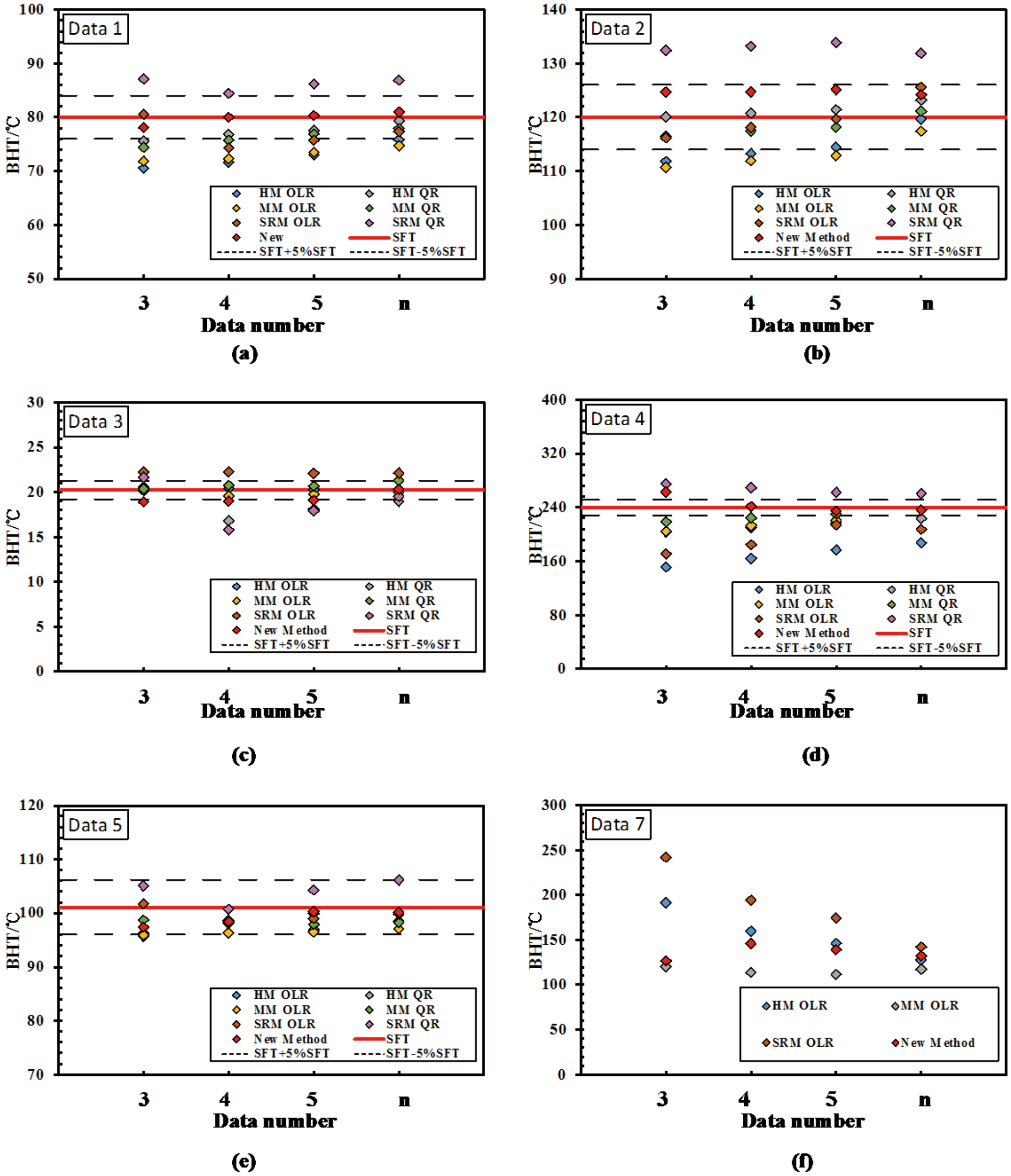


**Figure 6: SFT estimates of each method using the first 3, 4, 5 points or all data of a set, respectively.**

**Table 5: Deviation percentages of the SFT estimates using different methods.**

| Method | | Data 1 | | | | Data 2 | | | |
|---|---|---|---|---|---|---|---|---|---|
| | | Data number | | | | Data number | | | |
| | | 3 | 4 | 5 | all | 3 | 4 | 5 | all |
| HM | OLS | -11.756 | -10.378 | -8.765 | -5.161 | -6.808 | -5.583 | -4.608 | -0.283 |
| | QR | -5.456 | -3.944 | -3.058 | -0.785 | 0.067 | 0.658 | 1.217 | 2.717 |
| MM | OLS | -10.186 | -9.576 | -8.091 | -6.609 | -7.708 | -6.708 | -5.908 | -2.125 |
| | QR | -6.975 | -5.304 | -3.828 | -2.580 | -2.933 | -2.100 | -1.508 | 0.958 |
| SRM | OLS | 0.734 | -7.094 | -5.307 | -3.298 | -3.142 | -1.517 | -0.250 | 4.692 |
| | QR | 8.970 | 5.601 | 7.781 | 8.643 | 10.367 | 11.017 | 11.592 | 9.925 |
| Proposed method | | -2.367 | 0.028 | 0.470 | 1.249 | 3.929 | 3.971 | 4.289 | 3.527 |

| | | Data 3 | | | | Data 4 | | | | Data 5 | | | |
|---|---|---|---|---|---|---|---|---|---|---|---|---|---|
| | | Data number | | | | Data number | | | | Data number | | | |
| | | 3 | 4 | 5 | all | 3 | 4 | 5 | all | 3 | 4 | 5 | all |
| HM | OLS | 1.600 | 0.835 | 0.212 | 0.385 | -36.800 | -31.438 | -26.250 | -21.833 | -5.350 | -4.717 | -4.125 | -2.632 |
| | QR | 1.215 | -16.928 | -10.731 | -6.267 | -14.917 | -12.404 | -9.500 | -6.875 | -4.779 | -2.457 | -1.191 | -1.029 |
| MM | OLS | -0.435 | -3.289 | -2.528 | -1.220 | -14.583 | -11.029 | -8.067 | -8.067 | -5.123 | -4.740 | -4.602 | -4.017 |
| | QR | 0.652 | 2.588 | 2.074 | 5.195 | -8.842 | -6.358 | -3.896 | -3.896 | -2.332 | -2.546 | -3.131 | -2.822 |
| SRM | OLS | 9.852 | 9.931 | 9.151 | 9.294 | -28.617 | -22.992 | -10.754 | -13.588 | 0.613 | -2.937 | -2.070 | -1.238 |
| | QR | 6.963 | -22.089 | -11.501 | -3.709 | 14.696 | 12.213 | 9.367 | 8.696 | 3.907 | -0.386 | 3.106 | 4.995 |
| Proposed method | | -4.958 | -4.844 | -0.543 | 0.380 | 9.501 | 0.784 | -2.198 | -1.632 | -3.667 | -2.661 | -0.781 | -0.967 |

Both data quantity and method will affect the prediction accuracy, some methods at specific conditions may have better results than the proposed method. So Theil inequality coefficient (TIC), an overall evaluation, was used to further make the comparison. The value of TIC is in [0, 1] and could be used to make comparison among different data sets. For each method, the closer the TIC to zero, the more accurate the method. The results of Theil inequality coefficient (TIC) were shown in Figure 7. It can be seen that the new method is the only method that the TIC values of all data sets were less than 3%, indicating that the new method not only can estimate SFT from very few data accurately, but also stably.

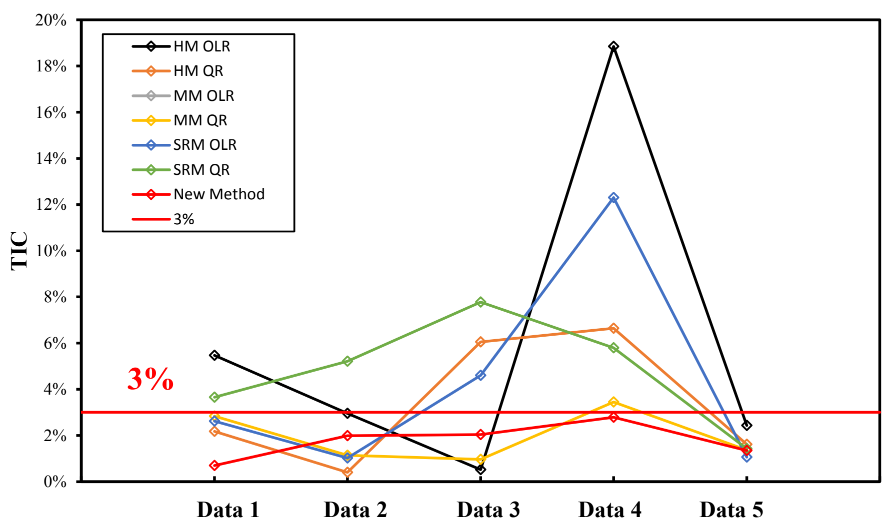


**Figure 7：Comparison of TIC values estimated by different methods**

## 5. CONCLUSIONS

(1) A modified method was proposed to estimate SFT from the BHT data and shut-in time.

(2) The estimation accuracy and fitting ability of the proposed method was verified using 8 BHT data sets, including synthetic data, geothermal, and petroleum field data.

(3) Comparison among different methods was also conducted. The proposed method can estimate SFT accurately and stably, even from a small number of BHT data.

## REFERENCES

Armstrong, P.A., Chapman, D.S., Funnell, R.H., Allis, R.G., and Kamp, P.J.J.: Thermal Modeling and Hydrocarbon Generation in an Active-margin Basin: Taranaki Basin, New Zealand. *Aapg Bulletin*, **80**, (1996), 1216-1241.

Ascencio, F., García, A., Rivera, J., and Arellano, V.: Estimation of Undisturbed Formation Temperatures under Spherical-radial Heat Flow Conditions, *Geothermics*, **23**, (1994), 317-326.

Bassam, A., Santoyo, E., Andaverde, J., Hernández, J.A., and Espinoza-Ojeda, O.M.: Estimation of Static Formation Temperatures in Geothermal Wells by Using an Artificial Neural Network Approach, *Computers & Geosciences*, **36**, (2010), 1191-1199.

Brennand, A.W.: A New Method for the Analysis of Static Formation Temperature Test, *Proceedings*, 6th New Zealand Geothermal Workshop, New Zealand (1984).

Cao, S., Lerche, I., and Hermanrud, C.: Formation Temperature Estimation by Inversion of Borehole Measurements, *Geophysics*, **53**, (2012), 979-988.

Chen, M. R., Li, X., Zhang, X., and Lu, Y. Z.: A Novel Particle Swarm Optimizer Hybridized with Extremal Optimization, *Applied Soft Computing*, **10**, (2010), 367-373.

Cooper, L.R., and Jones, C.: The Determination of Virgin Strata Temperatures from Observations in Deep Survey Boreholes, *Geophysical Journal International*, **2**, (1959), 116–131.

Dowdle, W.L., and Cobb, W.M.: Static Formation Temperature from Well Logs - an Empirical Method, *Journal of Petroleum Technology*, **27**, (1975), 1326-1330.

Espinoza-Ojeda, O.M., Santoyo, E., and Andaverde, J.: A New Look at the Statistical Assessment of Approximate and Rigorous Methods for the Estimation of Stabilized Formation Temperatures in Geothermal and Petroleum Wells, *Journal of Geophysics & Engineering*, **8**, (2011), 233-258(26).

Fomin, S., Chugunov, V., and Hashida, T.: Analytical Modelling of the Formation Temperature Stabilization during the Borehole Shut-in Period, *Geophysical Journal International*, **155,** (2003), 469-478.

Garcia, A., Hernandez, I., Espinosa, G., and Santoyo, E.: Temlopi: a Thermal Simulator for Estimation of Drilling Mud and Formation Temperatures during Drilling of Geothermal Wells, *Computers & Geosciences*, **24**, (1988), 465-477.

Hasan, A.R., Kabir, C.S., and Hasan, A.R.: Static Reservoir Temperature Determination from Transient Data after Mud Circulation, *SPE Drilling & Completion*, **9**, (1994), 17-24.

Jordehi, A.R.: A Review on Constraint Handling Strategies in Particle Swarm Optimization, *Neural Computing & Applications*, **26**, (2015), 1-11.

Kennedy, J., and Eberhart, R.: Particle Swarm Optimization. Neural Networks, 1995, *Proceedings*, IEEE International Conference (1995).

Kutasov, I.M., and Eppelbaum, L.V.: Determination of Formation Temperature from Bottom-hole Temperature Logs—a Generalized Horner Method, *Journal of Geophysics & Engineering*, **2**, (2005), 90-96.

Kutasov, I.M., Technologies, M.S., and Monica, S.: Applied Geothermics for Petroleum Engineers, *Journal of Petroleum Science and Engineering*, (1999).

Lech, P.J., Pappoe, R., Nakamura, T., and Russell, S.J.: The Temperature Stabilization of a Borehole, *Virology*, **46**, (2012), 1301-1303.

Li, D.X.: Non-linear Fitting Method of Finding Equilibrium Temperature from BHT Data, *Geothermics*, **15**, (1986), 657-664.

Mahor, A., and Rangnekar, S.: Short Term Generation Scheduling of Cascaded Hydroelectric System Using Novel Self-adaptive Inertia Weight PSO, *International Journal of Electrical Power & Energy Systems*, **34**, (2012), 1-9.

Manetti, G.: Attainment of Temperature Equilibrium in Holes during Drilling, *Geothermics*, **2**, (1973), 94–100.

Matthai, and Stephan, K.: Reservoir Simulation: Mathematical Techniques in Oil Recovery, *Geofluids*, **8**, (2008), 344-345.

Melton, C.E., and Giardini, A.A.: Petroleum Formation and the Thermal History of the Earth's Surface. Journal of Petroleum Geology, **7**, (1984), 303–312.

Saito, S., Sakuma, S., and Uchida, T.: Drilling Procedures, Techniques and Test RM Results for a 3.7 km Deep, 500 $^{o}$C Exploration Well, kakkonda, japan, *Geothermics*, **27**, (1998), 573-590.

Santoyo, E., Garcia, A., Espinosa, G., Hernandez, I., and Santoyo, S.: Static_temp: a Useful Computer Code for Calculating Static Formation Temperatures in Geothermal Wells, *Computers & Geosciences*, **26**, (2000), 201-217.

Schoeppel, R.J., and Gilarranz, S.: Use of Well Log Temperatures to Evaluate Regional Geothermal Gradients, *Journal of Petroleum Technology*, **18** (1966), 667–73.

Shen, P.Y., and Beck, A.E.: Stabilization of Bottom Hole Temperature with Finite Circulation Time and Fluid Flow, *Geophysical Journal of the Royal Astronomical Society*, **86**, (1986), 63-90.

Ziari, I., and Jalilian, A.: Optimal Placement and Sizing of Multiple APLCs Using a Modified Discrete PSO, *International Journal of Electrical Power & Energy Systems*, **43**, (2012), 630-639.